Progress In Electromagnetics Research C, Vol. 43, 67–78, 2013

OPTIMIZATION OF A QUASI LOSS LESS AIR-CAVITY INVERTED MICROSTRIP LINE FROM MICROWAVE TO MILLIMETER-WAVE FREQUENCIES AND COMPARISON WITH THE COPLANAR GOUBAU LINE AT 60 GHz

Marjorie Grzeskowiak[1, *], Julien Emond[1], Stephane Protat[1], Gaelle Lissorgues[2], Frederique Deshours[3], Elodie Richalot[1], and Odile Picon[1]

[1]Université Paris-Est, ESYCOM (EA 2552), UPEMLV, ESIEE-Paris, CNAM, F-77454 Marne-la-Vallée, France

[2]Université Paris-Est, ESYCOM (EA 2552), UPEMLV, ESIEE-Paris, CNAM, F-93162 Noisy-le-Grand, France

[3]UPMC Université Paris 06, L2E, 4 Place Jussieu, 75252 Paris Cedex 05, France

Abstract—An inverted micro-strip line (IML) is proposed at microwave and millimeter wave frequencies. This IML on high resistivity silicon (HRS) is studied from 10 to 100 GHz and presents an attenuation lower than 0.08 dB/mm on the whole frequency band. A parametric study, in order to minimize the attenuation and the dispersion of the inverted line in the 10–100 GHz bandwidth, is performed using numerical full wave calculations with HFSS (High Frequency Structural Simulator) tool. A complementary study is added: a large variety of characteristic impedances (for instance, from 38 Ω to 87 Ω at 60 GHz) is performed, the change of propagation modes is observed and the qualification and quantification of the losses allows minimizing them. A comparison with a line of the same length and width without ground plane, the Planar Goubau Line (PGL) is reported in the 10–100 GHz band and a first measure of the PGL is performed, in the 55–67 GHz band, presenting the same propagation mode as the IML at 60 GHz. The measured attenuation of 0.064 dB/mm in the 55–67 GHz obtained for the PGL promises a comparable value for the IML in the measured band.

Received 17 July 2013, Accepted 19 August 2013, Scheduled 28 August 2013

* Corresponding author: Marjorie Grzeskowiak (marjorie.grzeskowiak@univ-mlv.fr).

1. INTRODUCTION

The 57–66 GHz frequencies band is a European UWB bandwidth, dedicated to the Wireless Local Area Networks (WLAN), for its aspects of miniaturization, high-speed transmission rate and security, due to the atmospheric absorption in this frequencies band.

A state-of-art [1] summarizes the measured attenuation constants for different technologies on silicon for 50 Ohms lines. We can observe in this reference [1] as best result a minimum attenuation of 0.26 dB/mm at 60 GHz for a microstrip line ($w = 24\,\mu\text{m}$; $h = 10\,\mu\text{m}$) on BCB ($t = 2\,\mu\text{m}$ of copper). And a simulated result on a multilayer Low Resistivity Silicon using a suspended microstrip line [2] promises an attenuation of 0.13 dB/mm ($Z_c = 50\,\Omega$, $W = 900\,\mu\text{m}$) at 60 GHz. Other open structures, like CPWs on High Resistivity without the SiN layer between the center stripline and the two ground planes on both sides of the stripline, present attenuations constant less than 1 dB/mm up to 100 GHz, and particularly a measured value lower than 0.08 dB/mm at 60 GHz [3]. To prevent the penetration of the electric field of a coplanar line in the substrate in the case of low-resistivity silicon, a patterned ground shield is added beneath the line [4], and decreased the attenuation at 60 GHz from 1.141 dB/mm for conventional coplanar line to 0.731 dB/mm for the patterned ground shield coplanar line.

The inverted micro-strip line is dedicated to minimize the dielectric losses, because of the propagation of the waves in the vacuum instead of a dielectric substrate and assure to the electronic circuits to be protected from the undesired electromagnetic waves in a silicon-glass structures, like a self-packaging protection. The inverted micro-strip line on alumina sheet can be associated to a Micro-Hollow Cathode Sustained Discharge (MCSD) [5] to increase the interaction between the RF electromagnetic waves and the plasma discharge in comparison with a classical micro-strip line, where the RF electric field tends to be confined in the substrate instead of penetrating in the plasma. A micro-strip inverted line on Duroid 5880 using of artificial magnetic conductors (AMC), called micro-strip gap waveguide [6], improves the propagation of a quasi-TEM mode and avoids the propagation of all modes in forcing the RF electric field to stay along the line in the vacuum gap. The silicon-glass structure, with an anodic bonding technique, of simple process and low cost, can naturally encapsulate pressure sensors in the vacuum gap [7], and the protected package allows a operation of the sensors in high temperature environments, in comparison with the commercial sensors.

In this paper, we present a study on the inverted microstrip line up to 100 GHz and a simulated attenuation coefficient as low as 0.067 dB/mm is obtained at 60 GHz ($Z_c = 67\,\Omega$; $W = 100\,\mu\text{m}$; $h = 100\,\mu\text{m}$). In a first part, we describe the IML structure, and how a parametric study allows optimizing the attenuation and dispersion of the transmission line, versus the width of line (W) and cavity air-gap height (h). We can observe a change in the propagation mode in the 10–100 GHz band and the ground plane is found to be unnecessary above 50 GHz. We compare the IML structure with the structure without ground plane for the optimized width of line, which then corresponds to a PGL. As the technological process to fabricate a planar structure is simplified compared to the IML process, we can start preliminary measurements (on PGL) helpful to estimate performances of IML.

2. DESCRIPTION OF INVERTED MICROSTRIP LINE

In the Figure 1, the conductor line (W: width of conductor line; t: thickness of the conductor line = 1 μm; metal conductivity $\sigma = 3.810^7\,\text{S}\cdot\text{m}^{-1}$) is placed on the silicon substrate ($\varepsilon_r = 11.6$; $H_{silicon} = 500\,\mu\text{m}$), of high resistivity ($\sigma = 0.025\,\text{S}\cdot\text{m}^{-1}$).

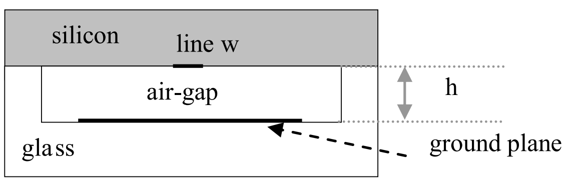

Figure 1. Cross view of the inverted line on HR Silicon.

The ground plane is printed on the glass substrate ($\varepsilon_r = 4$; $H_{glass} = 500\,\mu\text{m}$). In this structure, with an air cavity separating signal and ground, the electric field is confined in the air cavity, so the dielectric losses are minimized and the dispersion of the line parameters is decreased. This encapsulation of the line limits also the radiation of the line leading to minimized radiating losses. In a previous paper [8], we studied, fabricated and measured such a IML structure, and a very low attenuation was obtained for this line at 8 GHz ($\alpha = 0.02$ dB/mm for $h = 100\,\mu\text{m}$, $W = 368\,\mu\text{m}$ and $Z_c = 300\,\Omega$).

In the present study, simulations are carried out with HFSS, a full-wave simulator in order to reduce the attenuation of the line. We report on Figure 2 the attenuation (dB/mm) versus the air-cavity thickness for different W/h ratios at 60 GHz: each line has a constant w/h-value and the changing h-value, reported in the horizontal axis, implies

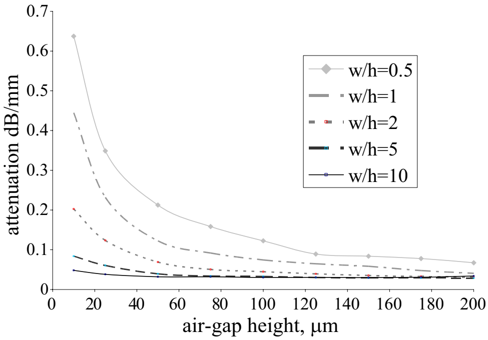

Figure 2. Attenuation (dB/mm) of the IML versus the air gap (10–200 μm) for different strip widths of conductor line (W/h from 0.5 to 10) at 60 GHz.

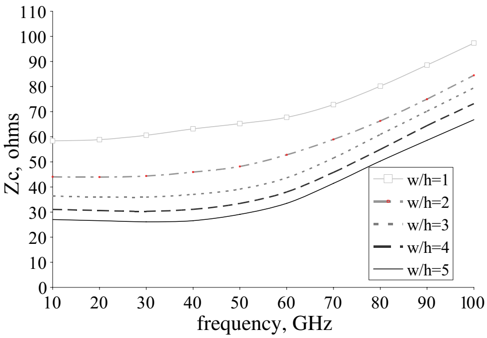

Figure 3. Characteristic impedance of the IML versus frequency for different W/h ratios ($h = 100\,\mu\text{m}$, $t = 1\,\mu\text{m}$).

that w is changing along one single line and curve. We notice the attenuation decreases with the air gap increase. It is clearly observed when this ratio is equal or inferior to 1.

An air-gap thickness of 100 μm should be chosen because of the easy technological aspect. On Figure 2, for a W/h ratio of 1, an air-gap thickness of 100 μm, the attenuation value is equal to 0.07 dB/mm at 60 GHz. In order to change the characteristic impedance, the W/h ratio is decreased to increase the characteristic impedance (Figure 3): each line has a constant w/h value but the gap thickness h, is constant and equal to 100 μm, and the strip width w, varies from 100 μm to 500 μm.

A wide range of characteristic impedance can be achieved without

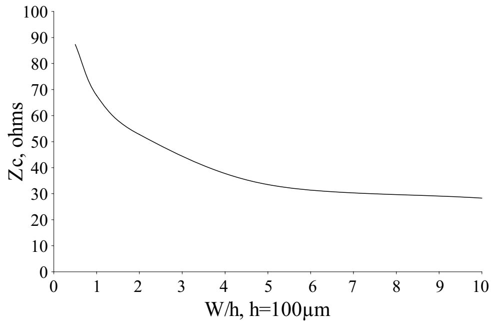

Figure 4. Characteristic impedance of the IML versus the width W ($h = 100\,\mu\text{m}$, $t = 1\,\mu\text{m}$).

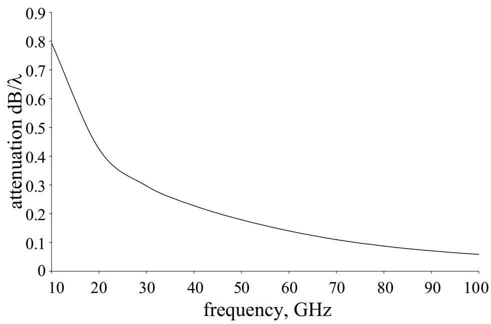

Figure 5. Attenuation (dB/λ) of the IML versus the frequency ($h = 100\,\mu\text{m}$, $W = 100\,\mu\text{m}$, $t = 1\,\mu\text{m}$) at 60 GHz.

a penalty in loss: for a fixed air-gap height of 100 μm (Figure 4), the characteristic impedance can be varied from 87 Ohms ($W/h = 0.5$) to 38 Ohms ($W/h = 5$). We can notice on Figures 2 and 4, that for $h = 100\,\mu\text{m}$, if the line width increases to 200 μm, the characteristic impedance is close to 50 Ω and the attenuation is lower than 0.07 dB/mm. The attenuation decreases when the characteristic impedance decreases, because of the line width increase.

In addition, the definition of the attenuation in dB per wavelength is also relevant: the necessary size of a component is inversely related to its intended frequency. At 60 GHz, a simulated attenuation of 0.14 dB/λ_g is performed (Figure 5) for $h = 100\,\mu\text{m}$ and $W = 100\,\mu\text{m}$.

To confirm the weak dispersion of this transmission line, we have reported the evolution of the imaginary propagation constant versus the frequency in the 10–100 GHz (Figure 6) and seen the linearity of

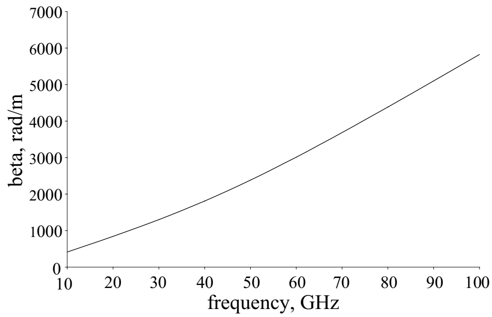

Figure 6. Phase-shift per unit length of the IML versus frequency.

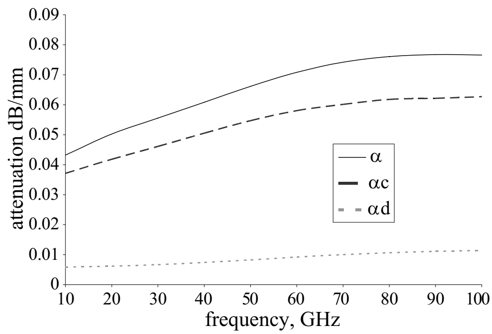

Figure 7. Attenuation (dB/mm) of the IML versus frequency (10–100 GHz) ($t_{strip} = 1\,\mu\text{m}$; $H_{silicon} = 500\,\mu\text{m}$; $W = 100\,\mu\text{m}$; $h = 100\,\mu\text{m}$) in considering total losses α, metallic losses α_c or dielectric losses α_d.

this parameter as a function of the frequency.

On the Figure 7, we can note a change of the total attenuation in slope with frequency: we deduce a propagation mode change. The different loss mechanisms of the IML can be quantified by separating the attenuation into conductor, dielectric and radiating components. In higher frequency, the losses are due essentially to the skin effect (conductor losses). To quantify and qualify the losses, we have considered many configurations of the IML structure; the first, with the dielectric losses ($\tan\delta_{glass} = 5 \cdot 10^{-4}$ and $\sigma_{silicon} = 0.025\,\text{S}\cdot\text{m}^{-1}$) with a finite conductivity for the gold line ($\sigma = 3.810^7\,\text{S}\cdot\text{m}^{-1}$) in free space, the second, with a perfect conductor, the third, with a perfect dielectric, and the fourth, in a metallic waveguide: we have deduced that the predominant losses are those of conductor. A mean to reduce the conductor losses is to increase the metallization thickness or the

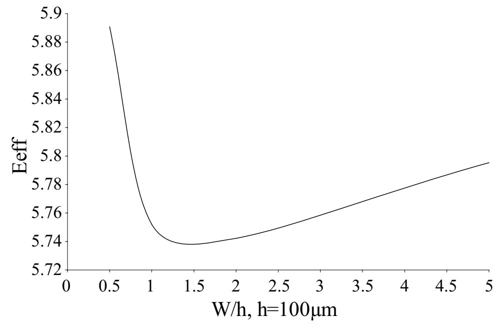

Figure 8. Effective permittivity for the IML ($h = 100\,\mu\text{m}$, $H_{silicon} = H_{glass} = 500\,\mu\text{m}$, $t = 1\,\mu\text{m}$) versus different W/h ratio (W/h from 0.5 to 5) at 60 GHz.

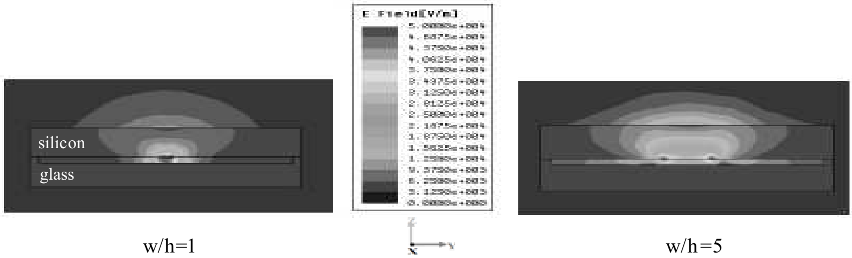

Figure 9. Electric field in magnitude in the transverse plane, for the IML ($h = 100\,\mu\text{m}$, $H_{silicon} = H_{glass} = 500\,\mu\text{m}$, $t = 1\,\mu\text{m}$) at 60 GHz for two W/h ratios ($W/h = 1$ and 5).

line width.

If we report the evolution of the effective permittivity versus the ratio W/h (Figure 8), we can observe a large change in slope between ratio smaller and higher than 2 that indicates that the propagation mode on the transmission line has changed. This phenomenon can be observed (Figure 9) on the cartography of the electric field for W/h ratio equal to 1 and 5.

3. COMPARISON BETWEEN PGL AND IML

The electric field distribution at 60 GHz (Figure 9) for $W/h = 1$ shows that the field is confined around the strip line at 60 GHz and that the field amplitude is very low on the ground plane.

As the ground plane is not influent in this case, we consider a transmission line on HRS substrate ($H = 500\,\mu\text{m}$, $W = 100\,\mu\text{m}$,

$t = 2\,\mu$m) without the ground plane. We already extensively studied and characterized this structure, called a Planar Goubau Line (PGL), in the 57–64 GHz band in a previous paper [9].

The PGL is used in the THz band [10]: the electromagnetic waves are confined on the strip of the PGL. This confinement can be improved by addition of corrugations [11]. The PGL can also realize passive structure like rejecters [12], interferometers [13], power-dividers [14, 15]. A configuration with reported active circuits on the PGL could be studied in the case of modulators and demodulators [16], as it is studied in other technological processes for the application Radio-on-Fiber (RoF) [17].

We compare the attenuation of the IML and of the PGL (Figure 10) versus the frequency in the 10–100 GHz band. The PGL is like a high-pass line and the PGL attenuation value is lower than 0.1 dB/mm when the frequency is higher than 40 GHz, contrary to the IML, where the attenuation stays lower than 0.08 dB/mm on the whole studied band. We can note a comparable value of the attenuations at 60 GHz (around 0.07 dB/mm) for both structures. In the IML case (Figure 11), the electric field below 40 GHz is confined in the substrate, whose dielectric losses are weak in HR Silicon.

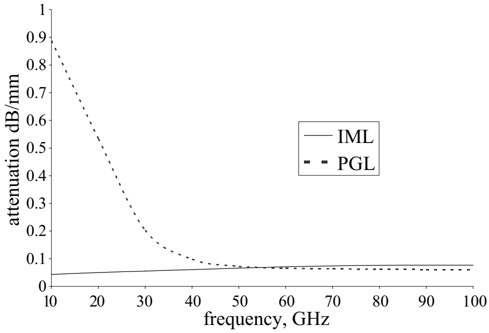

Figure 10. Attenuation of the PGL and inverted line versus the frequency ($h = 100\,\mu$m; $W = 100\,\mu$m; $t = 1\,\mu$m).

Due to the presence of Glass and Silicon substrates, which form an encapsulation of the line, the radiating losses are minimized. In the PGL case (Figures 10 and 12), the losses, essentially due to radiation, are very important below 40 GHz. The electric field distribution at 60 GHz is the same for the IML (Figure 11) and the PGL (Figure 12). For the PGL (Figure 12), when the frequency increases from 30 GHz to 90 GHz, the field is more and more confined around the strip line. According to these considerations, the PGL structure

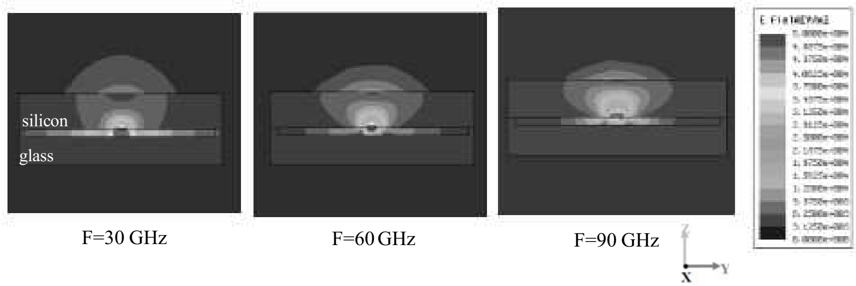

Figure 11. Cross view of magnitude electric field (V/m) of the inverted line on silicon at 30, 60 and 90 GHz.

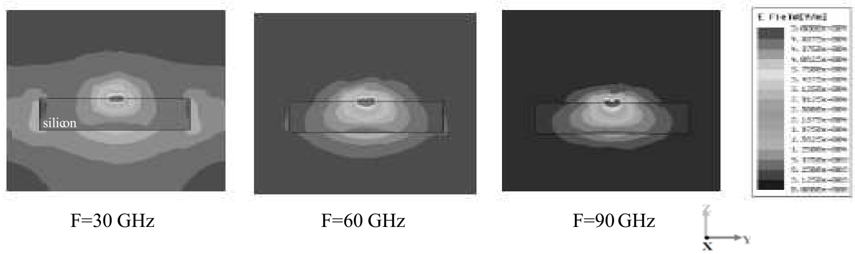

Figure 12. Cross view of magnitude electric field (V/m) of the PGL on silicon at 30, 60 and 90 GHz.

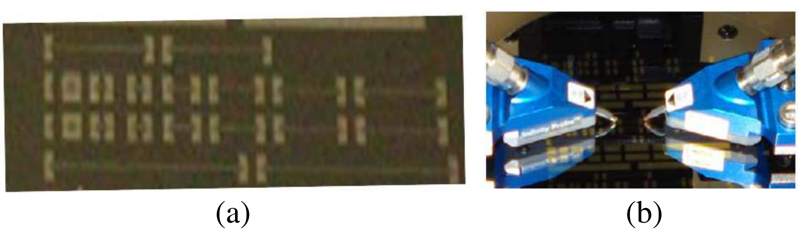

Figure 13. (a) Photograph of the PGL structures with (b) millimeter probes.

has been realized [9] (Figure 13(a)) because of its easier technological process only needing one mask level: the PGL structures have been characterized with a probe station equipped with millimeter probes in using a Microwave Network Analyzer (Figure 13(b)). A LRM (Line Reflect Match) calibration technique and an average of several similar measured structures are used respectively to eliminate the probing effect and the measurement setup and to minimize the influence of

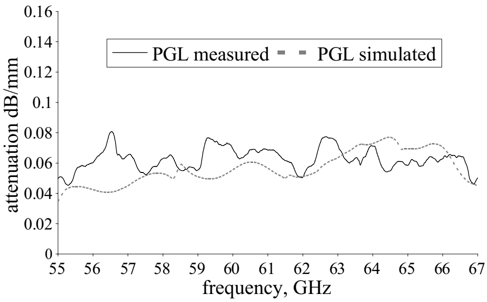

Figure 14. Measured and simulated attenuation of the PGL.

stochastic errors, positioning of the probes and others noises. The propagation constant is then extracted from the measured scattering parameters of a 20 mm-long line compared to those of each other line (PGL lengths of 2, 4, 6 and 10 mm), after the correct transmission of each back-to-back structure has been verified ($|S_{11}| < -15\,\mathrm{dB}$). An averaged attenuation value of 0.064 dB/mm in the 57–64 GHz band has been measured (Figure 14) from 20 extracted attenuations (redundancy for each length of line).

We suppose that a close value should be obtained for the equivalent IML structure in the same band, due to the correct prediction of the current 3D simulator, for instance the simulated and measured value of the PGL attenuation constant (Figure 14). This value offers the possibility to obtain capacitances and inductances of high quality factor ($Q = 183$ at 60 GHz) and so filters, antennas, loads, or power dividers.

4. CONCLUSION

Air gap offers, for the inverted micro-strip line, the weakest dielectric losses and a natural mechanical encapsulation protecting the device from any electromagnetic radiation. We have studied the behavior of the propagation (electric field, attenuation, dispersion) in the 10–100 GHz and an attenuation lower than 0.08 dB/mm is obtained by simulation on the whole frequency band. As for a W/h ratio below 2 the propagation mode is very similar to the one of a PGL, we have fabricated and characterized a PGL in the 57–64 GHz band. A 0.064 dB/mm attenuation for the PGL ($Z_c = 73\,\Omega$) in this band promises a close value for the IML: this value is lower than these of the state-of-art (a measured value of 0.26 dB/mm [1] and an expected value of 0.13 dB/mm [2] by simulation). The attenuation could also be reduced by a thicker line metallization or by increasing the line width and so decreasing the characteristic impedance.

REFERENCES

1. Belot, D., "Millimeter-wave design in silicon technologies," *Silicon Integrated Circuits in RF Systems*, 232–238, 2010.
2. Prasad, M., A. S. Gaur, V. K. Sharma, and N. P. Pathak, "Dispersion and attenuation characteristics of suspended microstrip line on multilayer lossy silicon substrate at 60 GHz," *International Conference on Infrared, Millimeter and THz Waves (2008)*, 1–2, 2008.
3. Makita, T., I. Tamai, and S. Seki, "Coplanar waveguides on high-resistivity silicon substrates with attenuation constant lower than 1 dB/mm for microwave and millimeter-wave bands," *IEEE Trans. on Electron Devices*, Vol. 58, No. 3, Mar. 2011.
4. Mat, D. A. A., R. K. Pokharel, R. Sapawi, H. Kanaya, and K. Yoshida, "Low-loss 60 GHz patterned ground shield CPW transmission line," *IEEE TENCON*, 1118–1121, 2011.
5. Pizarro, F., R. Pascaud, O. Pascal, T. Callegari, and L. Liard, "Experimental study of RF/microplasma interaction using an inverted microstrip line," *European Conference on Antennas and Propagation*, 1187–1190, 2013.
6. Pucci, E., A. U. Zaman, E. Rajo-Iglesias, and P-S. Kildal, "New loss loss inverted microstrip line using gap waveguide technology for slot antenna applications," *European Conference on Antennas and Propagation*, 979–982, 2011.
7. San, H., Y. Li, Z. Song, Y. Yu, and X. Chen, "Self-packaging fabrication of silicon-glass-based piezoresistive pressure sensor," *IEEE Electron Devices Letters*, Vol. 34, No. 6, 789–791, Jun. 2013.
8. Martoglio, L., E. Richalot, G. Lissorgues, and O. Picon, "A wideband 3D-transition between coplanar and inverted microstrip on silicon to characterize a line in MEMS technology," *Microwave and Optical Technology Letters*, Vol. 46, No. 4, 378–381, Aug. 20, 2005.
9. Emond, J., M. Grzeskowiak, G. Lissorgues, S. Protat, F. Deshours, E. Richalot, and O. Picon, "A low planar Goubau line and a coplanar-PGL transition on high resistivity silicon substrate in the 57–64 GHz band," *Microwave and Optical Technological Letters*, Vol. 54, No. 1, 164–168, Jan. 2012.
10. Xu, Y. S. and R. G. Bosisio, "A study of planar Goubau lines (PGLS) for millimeter-and-submillimeter-wave integrated circuits

(ICS)," *Microwave and Optical Technological Letters*, Vol. 43, No. 4, 290–293, Nov. 2004.

11. Laurette, S., A. Treizebre, and B. Bocquet, "Corrugated Goubau lines to slow down and confine THz waves," *IEEE Transactions on Terahertz Science and Technology*, Vol. 2, No. 3, May 2012.
12. Treizebre, A., M. Hofman, and B. Bocquet, "Terahertz spiral planar Goubau line rejectors for biological characterization," *Progress In Electromagnetics Research M*, Vol. 14, 163–176, 2010.
13. Laurette, S., A. Treizebre, N.-E. Bourzgui, and B. Bocquet, "Terahertz interferometer Goubau-line waveguides," *Progress In Electromagnetics Research Letters*, Vol. 30, 49–58, 2012.
14. Xu, Y. S., C. Nerguizian, and R. G. Bosisio, "Wideband planar Goubau line integrated circuit components at millimeter waves," *IET Microwave Antennas Propagation*, Vol. 5, No. 8, 882–885, Jun. 2011.
15. Treizebre, A., S. Laurette, Y. Xu, R. G. Bosisio, and B. Bocquet, "THz power divider circuits on planar Goubau lines (PGLs)," *Progress In Electromagnetics Research C*, Vol. 26, 219–228, 2012.
16. Karim, M. K., M. Sun, L. C. Ong, and Y. X. Guo, "SiP-based 60 GHz transmitter in LTCC," *IEEE International Symposium on Radio-frequency Integration Technology (RFIT)*, 13–15, Nov. 2012.
17. Cao, Z., C. M. Okonkwo, H. P. A. van den Boom, B. Yang, S. Zou, M. Huang, E. Tangdiongga, and A. M. J. Koonen, "Simple and low cost remote-up conversion scheme using only one optical modulator and its application in a 60 GHz radio-over-fiber system," *European Conference on Networks and Optical Communications (NOC)*, 1–4, 2012.